Available online at www.sciencedirect.com
ScienceDirect
Biomaterials 29 (2008) 1713–1719
Biomaterials
www.elsevier.com/locate/biomaterials

Incorporation of a matrix metalloproteinase-sensitive substrate into self-assembling peptides – A model for biofunctional scaffolds

Ying Chau [a], Ying Luo [h], Alex C.Y. Cheung [a], Yusuke Nagai [c], Shuguang Zhang [d,e], James B. Kobler [f,g], Steven M. Zeitels [f,g], Robert Langer [b,*]

[a] Department of Chemical Engineering, The Hong Kong University of Science and Technology, Clear Water Bay, Hong Kong, China
[b] Department of Chemical Engineering, Massachusetts Institute of Technology, 77 Massachusetts Avenue, E25-342, Cambridge, MA 02139, USA
[c] Menicon Co., Ltd., 5-1-10 Takamoridai, Kasugai, Aichi 487-0032, Japan
[d] Center for Biomedical Engineering, Massachusetts Institute of Technology, 77 Massachusetts Avenue, NE47-379, Cambridge, MA 02139, USA
[e] Center for Bits and Atoms, Massachusetts Institute of Technology, 77 Massachusetts Avenue, Cambridge, MA 02139, USA
[f] Department of Surgery, Harvard Medical School, Boston, MA, USA
[g] Center for Laryngeal Surgery and Voice Rehabilitation, Massachusetts General Hospital, One Bowdoin Square, 11th floor, Boston, MA 02114, USA
[h] Department of Biomedical Engineering, Peking University, 60 Yan-Nan Yuan, HaiDian District, Beijing, China

Received 29 May 2007; accepted 6 November 2007
Available online 14 January 2008

Abstract

Controlling and guiding cell behavior requires scaffolding materials capable of programming the three-dimensional (3-D) extracellular environment. In this study, we devised a new self-assembling peptide template for synthesizing nanofibrous hydrogels containing cell-responsive ligands. In particular, the insertion of a matrix metalloproteinase-2 (MMP-2) labile hexapeptide into the self-assembling building blocks of arginine-alanine-aspartate-alanine (RADA) was investigated. A series of peptides, varied by the position of the MMP-2 hexapeptide substrate and the length of RADA blocks, were prepared by parallel synthesis. Their self-assembling capabilities were characterized and compared by circular dichroism spectroscopy and dynamical mechanical analysis. Among all the different insertion patterns, the sequence comprising a centrically positioned MMP-2 substrate was flanked with three RADA units on each side self-assembled into a hydrogel matrix, with mechanical properties and nanofiber morphology comparable to the native material built with $(RADA)_4$ alone. Exposure of the new gel to MMP-2 resulted in peptide cleavage, as confirmed by mass spectroscopy, and a decrease in surface hardness, as detected by nanoindentor, indicating that the enzyme mediated degradation was localized to the gel surface. The new design can be used for introducing biological functions into self-assembling peptides to create scaffolding materials with potential applications in areas such as tissue engineering and regenerative medicine.

Keywords: Self-assembly; Peptide; Biomimetic material; Matrix metalloproteinase; Nanofiber; Hydrogel

1. Introduction

The natural extracellular matrix (ECM) contains a plethora of signals that synergistically activate various intracellular signaling pathways to control and guide the cell behavior. Recapitulating the ECM regulatory mechanisms is of central importance in fundamental cell studies and cell-based applications such as tissue engineering. Methods have been established to capture the nano-topographical and biochemical characteristics in the natural ECM [1,2]. Most of these methods, however, entail chemical syntheses that lack an adequate flexibility to generate tunable biochemical patterns for the rational design of extracellular environment. In addition, a thorough and comprehensive understanding of ECM–cell interactions and the screening of biomaterials may involve high-throughput studies that require systematically varying material and biochemical properties in a facile way [3,4]. We explore here a pure peptide-based platform for

* Corresponding author. Tel.: +1 617 253 3107; fax: +1 617 258 8827.
E-mail address: rlanger@mit.edu (R. Langer).

0142-9612/$ - see front matter © 2007 Elsevier Ltd. All rights reserved.
doi:10.1016/j.biomaterials.2007.11.046

enriching biological functions in self-assembling three-dimensional (3-D) scaffolds. A new family of biofunctional materials can potentially be obtained from automated peptide synthesis.

Self-assembling peptides (SAPs) have recently emerged as an attractive class of 3-D scaffolding materials, mainly due to their nano-scale fibrous and porous topographies that mimic the natural ECM features [5–8]. Among them, peptides (arginine-alanine-aspartate-alanine)$_4$ ((RADA)$_4$) have been used to form scaffolds *in situ* for tissue engineering applications [9–11]. This material has been shown to support the growth and differentiation of a variety of cells, including those originated from human, mammals, mouse and chicken, and covering stem cells, progenitor cells and established cell lines [12]. We reason that cell behavior can be further controlled by cell–material interactions if biofunctions are synthesized into the peptide scaffolds. Thus, we investigated a new SAP template that consists of two modules: one for generating ordered secondary structures to enable hydrogel formation, and the other for supplying biological cues to elicit specific cellular responses.

Cellular adhesion ligands, such as arginine-glycine-aspartate (RGD) from fibronectin and tyrosine-isoleucine-glycine-serine-arginine (YIGSR) from laminin, have been widely used in the tissue-scaffold design to enhance cell attachment and other basic functions [13]. In order to further direct cell behavior, it is necessary to incorporate additional signals on the scaffold to communicate with cells as they remodel the extracellular matrix (ECM) [1]. More recently, oligopeptides that are sensitive to the enzymatic cleavage of matrix metalloproteinases (MMPs) have been added to synthetic polymers and peptide-amphiphiles [14,15]. MMPs belong to a family of proteases that degrade ECM components and therefore play important roles in tissue regeneration. They make way for cells to expand, allow the ECM to be remodeled, and release embedded growth factors and other signals from the ECM to stimulate cell differentiation and tissue growth [16,17]. Incorporating MMP-cleavable substrates into SAPs is an attractive strategy to engineer a dynamic mechanism for eliciting cell and tissue remodeling activities [1].

To synthesize SAPs prone to remodeling by ECM proteases, we inserted an MMP-2 cleavable sequence, proline-valine-glycine-leucine-isoleucine-glycine (PVGLIG) into an SAP. This hexapeptide was selected from screening a combinatorial peptide library for optimal MMP substrates [18]. Its specificity and sensitivity was previously demonstrated in an MMP-sensitive polymer–peptide–drug conjugate [19]. The optimal placement of PVGLIG within an SAP was studied by synthesizing a series of peptides with varied PVGLIG positioning and RADA block length. The self-assembling and gelling capabilities of the resulting materials were compared and characterized by dynamical mechanical analysis (DMA), circular dichroism (CD) spectroscopy and atomic force microscopy (AFM). The MMP-mediated degradation of the selected PVGLIG-containing SAP was studied by a fluorescence detection assay, mass spectroscopic analysis and nanoindentation analysis.

2. Materials and methods

2.1. Parallel peptide synthesis

Peptides were synthesized by the Biopolymers Laboratory at the Massachusetts Institute of Technology using a multiple peptide synthesizer (Intavis, Koeln, Germany). Standard FMOC (9-Fluorenylmethoxycarbonyl) procedures were followed and O-(7-azabenzotriazol-1-yl)-1,1,3,3-tetramethyluronium hexafluorophosphate (HATU) was used as the coupling reagent. All the peptides in this study have an acetylated N-terminus and an amidated C-terminus. Their identity was confirmed by matrix-assisted laser desorption/ionization time-of-flight (MALDI-TOF) mass spectroscopy. Typically, one batch of synthesis gave a yield of 1–10 mg of crude product for each programmed peptide sequence. The crude peptides were dissolved in deionized water at 5 mg/ml, sonicated for an hour and centrifuged at 8000 rpm (5415C, Eppendorf, Westbury, NY). Any precipitate was discarded and the supernatant was retained and lyophilized. This peptide product was used for mechanical and spectroscopic characterization. Peptides used for AFM imaging and fluorescence detection assay were further purified by reversed-phase HPLC over a gradient of 0–100% acetonitrile containing 0.2% trifluoroacetic acid (TFA) on a C-18 column (Vydac, Hesperia, CA). The final purity was $\geq$80% according to the result of analytical HPLC assays.

2.2. Circular dichroism spectroscopy

Secondary structures were analyzed by measuring ellipticity spectra from 250 to 190 nm using a CD spectrometer (model 202, Aviv, Lakewood, NJ). Each peptide was first dissolved at 1% (10 mg/ml) in deionized water, sonicated for at least 30 min and left to stand overnight. The peptide solution was then diluted to 0.01–0.05% with deionized water and pipetted into a cuvette with 1 mm path length for acquiring spectra. A blank reference of water was subtracted from the raw data before molar ellipticity was calculated. The calculation was based on the formula: $[\theta]_\lambda = \theta_{obs} \times 1/(10Lcn)$, where $[\theta]_\lambda$ = molar ellipticity at λ in deg cm^2 d/mol, θ_{obs} = observed ellipticity at λ in mdeg, L = path length in cm, c = concentration of peptide in M, and n = number of amino acids in the peptide.

2.3. Dynamical mechanical analysis

To analyze the gellability and the bulk mechanical properties of peptides, dynamic shear experiments were performed in a cone–plate geometry (cone with 2 cm diameter and 2° angle) using a rheometer (AR2000, TA Instrument, New Castle, DE). The peptide was dissolved in deionized water at 1% (10 mg/ml), sonicated for at least 30 min and left to stand overnight, giving time for the self-assembling process (if present) to proceed. Eighty microliters of aliquot was pipetted onto the center of the peltier plate. The cone was lowered to an instrument with a default gap of 58 microns, and an oscillatory frequency sweep was performed from 1 to 10 Hz with 1% shear strain to record the storage modulus G' (characterizing the elastic behavior) and loss modulus G'' (characterizing the viscous property and energy dissipation) of the peptide solution. To induce gelation, 0.5 ml phosphate-buffered saline (PBS, pH 7.4) was applied to the periphery of the peptide solution without changing the confinement gap between the cone and plate. After 1 h, PBS on the periphery was blotted dry and the same frequency sweep was performed again to characterize the resulting aqueous peptide after PBS application. To analyze the change in the bulk mechanical property due to enzymatic digestion, PBS containing 50 nM MMP-2 was applied to the periphery for 24 h. The enzyme solution was blotted dry before the frequency sweep was performed. (More details are provided in Supplementary information 3.)

2.4. Atomic force microscopy

Each peptide was first dissolved at 1% (10 mg/ml) in deionized water, sonicated for at least 30 min and allowed to stand overnight to allow time for the self-assembling process (if present). The peptide solution was then diluted to 100 μg/ml with deionized water. One microliter sample was loaded

onto a clean mica surface and air-dried overnight in a covered holder. Images with a resolution of 512 × 512 pixels were obtained by an AFM microscope (Nanoscope-MultiMode/Dimension, Digital Instruments, Santa Barbara, CA) running in a tapping mode. Silicon probes with a tip radius of 10–15 nm, a resonance frequency of 200 kHz and a spring constant of 3 N/m were used (Nanosensors probe, Neuchatel, Switzerland).

2.5. Enzymatic degradation of peptide solution by matrix metalloproteinase

Each peptide solution at 1% in water was diluted 10-fold further with Dulbecco's phosphate-buffered saline (DPBS) containing calcium and magnesium (Invitrogen, Carlsbad, CA). Recombinant active human MMP-2 (Calbiochem, San Diego, CA) was added to each peptide solution to a final concentration of 50 nM. For controls, the same volume of DPBS was added instead of the enzyme. Samples were incubated at 37 °C for 24 h. The extent of enzymatic digestion was analyzed by measuring the fluorescence yielded from reacting fluorescamine (97% pure, Sigma, St. Louis, MO) with free N-terminals produced by enzymatic cleavage. After incubation, two parts of fluorescamine solution, which was prepared as a 40 mM stock in acetone and diluted to 5 mM with DPBS just before use, was added to one part of each sample. Fluorescence was measured immediately using a plate reader (SpectraMax, Molecular Devices, Sunnyvale, CA) with an excitation wavelength of 355 nm and an emission wavelength of 460 nm. Serial dilutions of glycine–glycine solution were used as standards to correlate the fluorescence signals and the concentrations of free amines. The percentage cleavage was determined by this formula:

$$\text{Percentage cleavage} = \frac{\text{Concentration of free amines in peptide solution after incubation with MMP-2} - \text{Concentration of free amines in peptide solution without enzyme}}{\text{Concentration of peptide in solution calculated from mass and volume}} \times 100\%$$

2.6. Enzymatic degradation of peptide gel by matrix metalloproteinase

We first prepared a gel sample by dissolving the peptide in water at 1% w/v and keeping the solution at room temperature until viscous. PBS was gently applied on top of the peptide solution to initiate the gelation process. After 1 h, PBS was removed and the resulting hydrogel was used in the digestion experiments.

The degradability of the self-assembled peptide hydrogel was qualitatively investigated by mass spectroscopic analysis. The preformed hydrogel composed of 1% peptide was submerged in PBS containing 50 nM MMP-2 at a 1:9 volume ratio. The mixture was incubated at room temperature for 24 h. The composition of the solid gel was then subjected to qualitative analysis by ESI-TOF (QSTAR XL Mass Spectrometry System, Applied Biosystems, USA).

The change in the gel surface due to MMP-2 treatment was analyzed by a nanoindentor (CSM Instruments SA, Peseux, Switzerland) equipped with a Berkovich tip. A thin piece of the preformed hydrogel was sliced and placed on the glass slide. The load-displacement measurement was performed with a loading rate of 3 mN/s to a maximum load of 1 mN, followed by a holding time of 60 s, and an unloading rate of 3 mN/s. After the initial measurement, 10 μl of PBS containing 0.5 mg/ml MMP-2 was added on top of the gel piece. For the control experiment, the same volume of PBS was added instead of enzyme. A cap with Vaseline® surrounding the edge was put on the glass slide to prevent dehydration. After 24 h of incubation with the enzyme solution or blank PBS, the load-displacement curve was measured again by probing within 20 nm from the same point on the gel sample. We reported the fold difference in contact depth and surface hardness compared to the initial measurement. As the gel has a relatively rough surface, and surface unevenness introduces a large variation to the nanoindentation measurement, reporting the fold difference at the same location is more meaningful than the absolute values in revealing the real trend.

In analyzing the data, correction has been made to account for the viscoelasticity of the hydrogel based on the method developed by Ngan and coworkers [20].

3. Results

To investigate how the insertion of a biofunctional sequence would affect the self-assembling process, we synthesized a series of peptides containing an MMP-labile sequence, PVGLIG, and systematically varied the length of the flanking RADA units. For nomenclature, the peptides were designated as [*m*, *n*], with *m* and *n* indicating the number of RADA units bonded to the amino and carboxyl end of PVGLIG, respectively. Flanking arms containing 2–4 RADA units were studied.

Self-assembling of RADA peptides is initiated in water with the formation of beta-sheets, driven by the hydrophobic and charge interactions of the amino acid constituents. Profiling the secondary structures of the PVGLIG-containing peptides by CD spectroscopy and examining the existence of beta-sheets can provide basic information to understand the assembling capability of the peptides. The CD spectra of beta-sheets are typically characterized by a minimum at 216 nm and a maximum at 195 nm, while those of random coils a maximum at 218 nm and a minimum at 198 nm [21]. By comparing our data with the CD spectra of polylysine containing varying amounts of secondary structures [21], we found that all the PVGLIG-containing peptides showed mixed structures of beta-sheets and random coils (Fig. 1a, b). However, among these samples, [3, 3] and [4, 4] (Fig. 1a) had distinctively different CD curves with a trough at 216 nm indicating that the beta-sheet content was more than 50%. In contrast, the shortest sample [2, 2] and those peptides with unequal numbers of the flanking RADA units all showed a trough at 198 nm (Fig. 1b), indicating a more pronounced ratio of random coil over beta-sheet conformation adopted by the peptide chains. The CD spectrum of $(RADA)_4$ was consistent with the known fact that this peptide had a dominant beta-sheet content (Fig. 1c). It is noted that both [3, 3] and [4, 4] had a smaller molar ellipticity at 216 nm compared to $(RADA)_4$, suggestive of a lower beta-sheet content and more mixed secondary structures in the functionalized SAPs.

As indicated by the CD spectra, [3, 3] and [4, 4] have a higher beta-sheet content than the other PVGLIG-containing peptides. We expect that a dominance of ordered secondary structure is a prerequisite for the formation of nanofibers in water and the subsequent salt-induced gelation. The dependence of the peptide gellability on PVGLIG insertion pattern was further characterized by DMA (Table 1). An oscillatory frequency sweep (frequency = 1–10 rad/s) was performed to measure the storage modulus G' and the loss modulus G''.

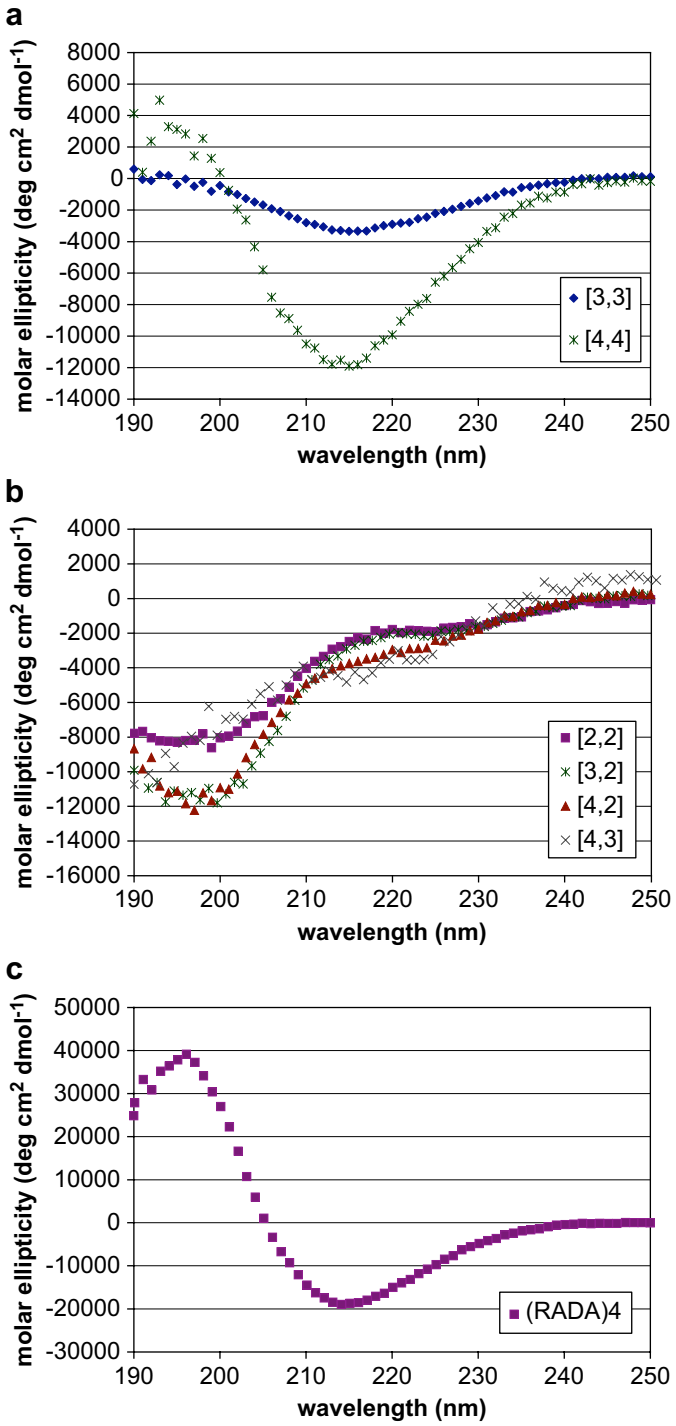

Fig. 1. CD spectra of 0.1% peptide solutions in water: (a) PVGLIG-containing peptides with a majority of beta-sheet structure, (b) PVGLIG-containing peptides with a majority of random coil structure, and (c) $(RADA)_4$.

The loss angle, δ, reflecting the ratio of G' to G'', quantifies the balance between mechanical energy storage and loss. When solid properties dominate over liquid properties, G' is larger than G'' and δ is less than 45°. Within the low frequency range, a relatively stable G' can be observed and the sample is defined as a gel. The PVGLIG-containing peptides dissolved in water resulted in solutions with different viscosities after an overnight equilibrium (by visual observation), but all samples remained as liquid capable of flowing. The increase in viscosity in water is related to the growth of nanofiber from the self-assembling peptides. PBS was subsequently used to promote the physical crosslinking of self-assembled peptides resulting in gelation. Among the samples tested, [3, 3] exhibited a small δ with consistent storage moduli (G') higher than 1 kPa over a range of different frequencies (data averaged over 1–10 Hz). The storage moduli were smaller than the original $(RADA)_4$. Besides [3, 3], [4, 4] also showed solid properties – the storage moduli, however, were one order of magnitude lower than [3, 3] and $(RADA)_4$. The resulting gel as a consequence was not strong enough and could hardly maintain a certain physical shape for practical use. The remaining peptides with PVGLIG insertion, including [2, 2], [3, 2], [4, 2] and [4, 3], did not form gels in PBS solution; they all had negligible storage moduli close to zero. Since the storage moduli for these peptides were too small to be detected accurately by the DMA instrument, the averaged G' values had a high noise-to-signal ratio and exhibited a large standard deviation.

Table 1
Average storage modulus (G') and loss angle (δ) of PVGLIG-containing peptides

$(RADA)_m$PVGLIG$(RADA)_n$ with values of [m, n] as listed	Gellability	δ (degree)	G′ (Pa)
[4, 4]	+	**6.2 ± 2.0**	**214.4 ± 47.6**
[4, 3]	–	100.8 ± 100	−1.9 ± 4.9
[4, 2]	–	126.7 ± 2.0	−1.5 ± 2.1
[3, 3]	+	**5.8 ± 0.2**	**1252.0 ± 62.5**
[3, 2]	–	110.0 ± 37.4	−0.3 ± 4.5
[2, 2]	–	132.9 ± 29.3	−1.6 ± 3.5
$(RADA)_4$	+	**2.9 ± 0.2**	**1541.7 ± 72.2**

Average ± standard deviation over 1–10 Hz with $n = 2$; gellable peptides are highlighted in bold.

By characterizing and comparing the rheological and CD properties, the [3, 3] peptide was found to have optimal self-assembling and mechanical properties. With three repeats of RADA flanking on each side of the MMP substrate, $(RADA)_3$PVGLIG$(RADA)_3$, or [3, 3] in short, consists of 30 amino acids and has an extended amide backbone of length around 10 nm. Macroscopically, we observed the formation of a hydrogel from this peptide by both visual observation and DMA. Morphological characterization was performed by tapping mode AFM to visualize the structural elements of the hydrogel matrix. The AFM image confirmed the formation of nanofibers in dilute aqueous condition (Fig. 2a). When plated at the same weight concentration, the fiber density of [3, 3] was notably lower compared to $(RADA)_4$ (Fig. 2b). As a negative control, we imaged [2, 2], a peptide containing majority random coil in its secondary structure and failing to gel in the presence of PBS. No fiber formation was observed for [2, 2].

To study the cleavability of $(RADA)_3$PVGLIG$(RADA)_3$ by MMP, an enzymatic digestion experiment based on a fluorescence assay was performed on peptide solution samples. Several peptides built with the same sequence template containing arbitrarily selected insertions, as well as $(RADA)_4$, were used as negative controls. Complete enzymatic cleavage occurred

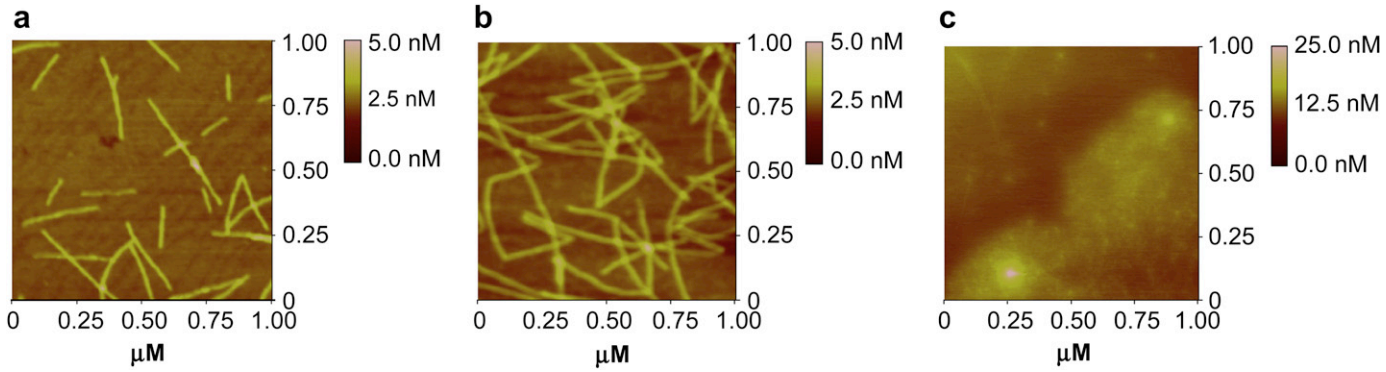

Fig. 2. AFM images of the peptides (a) $(RADA)_3PVGLIG(RADA)_3$, (b) $(RADA)_4$, and (c) $(RADA)_2PVGLIG(RADA)_2$. The first two peptides self-assemble into nanofibers in water while the last one is incapable of fiber formation. A 1×1 μm field is shown for each peptide. The gradient scale bars next to each frame spans a Z (height) range from 0 to 5.0 nm (a and b) and 0 to 8 nm (c).

after incubating the PVGLIG-containing peptide solution with MMP-2 for 24 h (Table 2). In comparison, an insignificant extent of cleavage was observed for all the control peptides. Therefore, MMP digestion is specific to $(RADA)_3PVGLIG(RADA)_3$. Further mass spectroscopic analysis on the degradation products confirmed that MMP-2 cleaved between PVG and LIG and produced $(RADA)_3PVG$ and $LIG(RADA)_3$ (Supplementary Information 1). The scissile bond position is consistent with the substrate specificity of MMP-2, which prefers proline in the P3 position, glycine in the P1 position, and leucine in the P1′ position [22].

To study the degradability of [3, 3] in the gel state, preformed [3, 3] matrices were immersed in PBS containing MMP-2, and the peptide degradation was investigated qualitatively by mass spectroscopy. After 24 h, all samples remained as solid gels without any noticeable change in size. The mass spectroscopic analysis of gel samples revealed that in addition to the peak representing uncleaved [3, 3] peptide (found MW = 3076.5, cal. MW = 3076.3 acetylated N-terminal and amidated C-terminal), there were two peaks at 1553.6 and 1540.8, respectively, corresponding to the cleavage fragments ($(RADA)_3PVG$ [cal. MW = 1553.7; acetylated N-terminal] and $LIG(RADA)_3$ [cal. MW = 1540.7; amidated C-terminal]. The presence of cleavage products suggested that the self-assembled [3, 3] peptide was attackable by MMP-2 enzyme.

After being exposed to MMP-2 for 24 h, [3, 3] gel did not show any significant change in the mechanical strength in terms of the average storage modulus (Supplementary Information 3). Although the enzymatic digestion did not cause a change in the bulk mechanical property, a change in the surface mechanical property was obvious. It led to an increase in the contact depth to about 2 μm by the nanoindentor tip at a given maximum load (1 mN in our method). As a result of the digestion, there was a significant decrease in the surface hardness (Table 3), where surface hardness is defined as the maximum load (P_{max}) divided by the projected contact area (A) between the indenter tip and the sample at maximum load.

4. Discussion

The "bottom up" approach is an important concept in modern material design, as it offers potential to construct novel sophisticated materials from simple building blocks [5,23]. However, it remains a challenge to understand how to assemble building blocks at the nano-/microscale to obtain desirable properties at the macroscopic level. In this study, we demonstrated a paradigm for building an MMP hexapeptide substrate into a self-assembling template made of ionic self-complementary peptides.

By investigating a variety of combination patterns of the MMP substrate and RADA self-assembling blocks, only one optimal sequence, $(RADA)_3PVGLIG(RADA)_3$, was identified useful for scaffold design. The factors that may affect the assembling of biofunctional peptides can be summarized. First, a majority beta-sheet assembling is a prerequisite for peptide's gellability and extended assembling blocks benefit the assembling process. This is supported by the fact that inserting PVGLIG into $(RADA)_4$ directly disrupted the assembling

Table 2
Cleavability of different peptides after incubating with MMP-2 for 24 h at 37 °C

Peptides	% Cleavage
$(RADA)_3$ PVGLIG $(RADA)_3$	106.66 ± 8.15
$(RADA)_4$	3.31 ± 0.85
$(RADA)_3$ YIGSR $(RADA)_3$	4.46 ± 2.89
$(RADA)_3$ GGGG $(RADA)_3$	0.27 ± 0.60
$(RADA)_3$ GGGGGGGG $(RADA)_3$	0.83 ± 0.65

Average ± standard deviation, $n = 2$.

Table 3
Effects of MMP-2 digestion on the surface mechanical properties of the self-assembling hydrogel formed by $(RADA)_3$ PVGLIG $(RADA)_3$

	Fold difference in contact depth	Fold difference in surface hardness
24 h Exposure to MMP-2	6.03 ± 1.97	0.035 ± 0.029
24 h Exposure to PBS (control)	1.15 ± 0.56	1.50 ± 1.86

Average ± standard deviation, $n = 3$.
Fold difference is the ratio of post-exposure measurement to pre-exposure measurement taken at the same point on the gel surface.

and resulted in a non-gellable peptide [2, 2]. Adding flanking RADA units gave rise to [3, 3] and [4, 4] with assembling and gelling capabilities. Second, the position of functional insertion has a determining effect on the peptide assembling properties. Comparing to [4, 3] or [4, 2], [3, 3] has a lower or equal mass ratio of RADA building blocks in the peptide chain. The superior assembling and gelling properties of [3, 3] can be attributed to the central position of PVGLIG. This speculation is also supported by another gellable sequence [4, 4], which has centrically positioned PVGLIG and showed secondary structures dominated by beta-sheet. However, by visual observation and by amino acid analysis (data not shown), [4, 4] had a very poor solubility in water, which may lead to its low value of storage modulus.

We propose a molecular model to help elucidate how peptide building blocks containing biofunctional sequence as insertion assemble, based on the assumption that these peptides form beta-sheet through non-covalent inter-molecular interactions similar to those in $(RADA)_4$. In Fig. 3, only a single sheet (instead of a double sheet) of [3, 3] is shown for clarity. The favorable interactions among the RADA units contribute to a decrease in enthalpy and these peptide sequences stack into a beta-sheet structure. We hypothesize that PVGLIG forms a random coil region. For the self-assembling process to be thermodynamically favorable, the enthalpic drive must be able to compensate the entropic penalty due to the incorporation of PVGLIG in the assembling blocks. This is consistent with our observation that there is a minimum requirement of the number of RADA units flanking the insertion sequence. A secondary premise in this model claims that the adjacent peptide strands are anti-parallel. This can possibly explain why sequences with unequal number of RADA units flanking on each side, such as [4, 3] and [4, 2], do not gel despite meeting the quantity requirement of RADA repeats. The extra RADA units cannot be favorably incorporated into the ordered region and the mismatch results in more random coil formation and increases the entropic penalty.

The assembly of the beta-sheet may involve sliding diffusion processes as proposed previously [24]. It took about 2 h for $(RADA)_4$ to re-assemble and restore the original fiber length after ultrasonic disruption of the nanofibers [24]. With the PVGLIG insertion, [3, 3] would presumably experience more molecular friction than pure $(RADA)_4$ during the peptide assembling process. This could cause slower nanofiber formation kinetics by [3, 3]. Indeed, we observed by visual inspection a difference between [3, 3] and $(RADA)_4$ in their rates to form viscous solutions in water. A solution containing 1% of $(RADA)_4$ appeared viscous immediately. In contrast, there was a lag time in the order of hours before the liquid turned viscous for the peptides containing PVGLIG. Since the inserted functional sequence mainly adopts a random coil conformation, the model would predict that the template pattern of [3, 3] discovered here is applicable to other bioactive peptides.

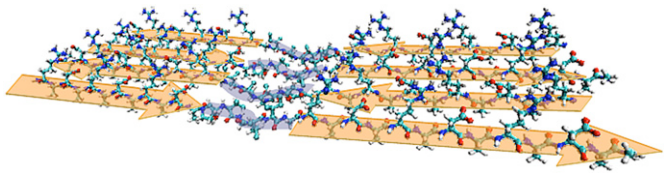

Fig. 3. A proposed beta-sheet assembling model for [3, 3] peptide, in which peptide chains align in anti-parallel directions, with a random coil region of PVGLIG (in blue bands) between RADA assemblies via energetically favorable interactions (in pink arrows). A single sheet with four beta-strands is shown for clarity.

Enzyme-sensitive hydrogels have been widely investigated for biomedical application such as drug delivery and tissue engineering. Only a few systems have so far been built on self-assembling materials, and how ordered structure would affect the digestion efficiency of an enzyme remains largely unknown. A gel made of a low molecular weight hydrogelators has shown that molecular stacking could prevent enzyme from attacking the target site located within assemblies [25,26]. Degradation only occurred after the assembled structure was disrupted and the constituent molecules released. In another amphiphilic peptide system containing MMP-sensitive sequences, degradation was observed [15]. These results indicate that the cleavage ability of an enzyme may vary with different forms of ordered structures. Pure ordered assemblies built from ionic self-complementary peptides were shown insusceptible to proteolytic degradation *in vitro* [27], probably due to the difficulty of the enzymes to penetrate the well-stacked fibrous structure.

Degradation occurred when an enzyme-sensitive sequence was incorporated in our SAP template. This observation is consistent with the proposed molecular model. Since the biofunctional sequences make up the loosely ordered random coil region, and so unlike the sequences protected within the ordered region, they are exposed and are susceptible to enzymatic attack. The [3, 3] hydrogel has a storage modulus over 1 kPa, much stronger than the gel made of amphiphilic peptides [15]. By inserting the PVGLIG segment instead of appending it to the terminal of an SAP, we intend MMP digestion to weaken the self-assembling gel, similar to the breakdown of ECM during tissue remodeling. Our CD and DMA studies showed that the degradation products alone had poor assembling capabilities (Supplementary Information 2), indicating that [3, 3] may not be able to maintain the mechanical integrity once cleaved by MMP. In our 24 h degradation study on the [3, 3] gel, enzymatic digestion was confirmed by the mass spectroscopic detection of cleavage fragments. We noticed that the digestion was localized to the surface of the gel, supported by the data that mechanical weakening was found in surface analysis (Table 3) but not bulk measurement (Supplementary Information 3). This is not surprising considering that the hydrogel assembled by ionic self-complementary peptides has small pores ranging from 5 to 200 nm [5] and presents a strong diffusion barrier for large enzymes such as MMP-2 (68 kDa). The localization of the enzymatic digestion to a surface front mimics proteolysis *in vivo*, in which ECM degradation is confined to the immediate pericellular environment [28]. To be more effective, cells concentrate

even soluble enzymes along the invasive front. For example, MMP-2 is activated by membrane-bound enzymes and inhibitors [29] and can dock on integrin-receptors on the cell surface [30]. It is through a highly regulated and confined proteolysis that cells can precisely orchestrate the dynamics and spatial orientation of ECM degradation.

5. Conclusions

New MMP-cleavable peptides capable of self-assembling into a nanofibrous scaffold hydrogel were synthesized. The material is responsive to MMP degradation and mimics the remodeling of natural ECM during tissue regeneration. This design template may also be used to synthesize other functional scaffolding materials with potential applications in areas such as tissue engineering and regenerative medicine.

Acknowledgements

We thank Richard Cook and Katie Tone for peptide synthesis, Hyoungshin Park, Frederick Tan and Rachel L. Williams from the Massachusetts Institute of Technology for technical assistance. Bing Tang and Alfonso Ngan from the University of Hong Kong have been kind to help us on the nanoindentation measurement and analysis. We are grateful to Amgen Inc. (Y. Chau), the Hong Kong Research Grants Council (Y. Chau and A.C.Y. Cheung), the Eugene B. Casey Foundation (Y. Luo), the Advisory Board Foundation (Y. Luo), and Menicon Co., Ltd. (Y. Nagai) for providing financial support.

Appendix. Supplementary material

Supplementary material can be found, in the online version, at doi:10.1016/j.biomaterials.2007.11.046

References

[1] Lutolf MP, Hubbell JA. Synthetic biomaterials as instructive extracellular microenvironments for morphogenesis in tissue engineering. Nat Biotechnol 2005;23(1):47–55.
[2] Stevens MM, George JH. Exploring and engineering the cell surface interface. Science 2005;310(5751):1135–8.
[3] Anderson DG, Levenberg S, Langer R. Nanoliter-scale synthesis of arrayed biomaterials and application to human embryonic stem cells. Nat Biotechnol 2004;22(7):863–6.
[4] Flaim CJ, Chien S, Bhatia SN. An extracellular matrix microarray for probing cellular differentiation. Nat Methods 2005;2(2):119–25.
[5] Zhang SG. Fabrication of novel biomaterials through molecular self-assembly. Nat Biotechnol 2003;21(10):1171–8.
[6] Stupp SI. Biomaterials for regenerative medicine. MRS Bull 2005;30(7):546–53.
[7] MacPhee CE, Woolfson DN. Engineered and designed peptide-based fibrous biomaterials. Curr Opin Solid State Mater Sci 2004;8(2):141–9.
[8] Holmes TC. Novel peptide-based biomaterial scaffolds for tissue engineering. Trends Biotechnol 2002;20(1):16–21.
[9] Holmes TC, de Lacalle S, Su X, Liu GS, Rich A, Zhang SG. Extensive neurite outgrowth and active synapse formation on self-assembling peptide scaffolds. Proc Natl Acad Sci U S A 2000;97(12):6728–33.
[10] Zhang SG, Holmes TC, Dipersio CM, Hynes RO, Su X, Rich A. Self-complementary oligopeptide matrices support mammalian-cell attachment. Biomaterials 1995;16(18):1385–93.
[11] Kisiday J, Jin M, Kurz B, Hung H, Semino C, Zhang S, et al. Self-assembling peptide hydrogel fosters chondrocyte extracellular matrix production and cell division: implications for cartilage tissue repair. Proc Natl Acad Sci U S A 2002;99(15):9996–10001.
[12] Zhao XJ, Zhang SG. Designer self-assembling peptide materials. Macromol Biosci 2007;7(1):13–22.
[13] Shin H, Jo S, Mikos AG. Biomimetic materials for tissue engineering. Biomaterials 2003;24(24):4353–64.
[14] Lutolf MP, Lauer-Fields JL, Schmoekel HG, Metters AT, Weber FE, Fields GB, et al. Synthetic matrix metalloproteinase-sensitive hydrogels for the conduction of tissue regeneration: engineering cell-invasion characteristics. Proc Natl Acad Sci U S A 2003;100(9):5413–8.
[15] Jun H-W, Yuwono V, Paramonov SE, Hartgerink JD. Enzyme-mediated degradation of peptide-amphiphile nanofiber networks. Adv Mater 2005;17(21):2612–7.
[16] Egeblad M, Werb Z. New functions for the matrix metalloproteinases in cancer progression. Nat Rev Cancer 2002;2(3):161–74.
[17] Woessner JF, Nagase H. Matrix metalloproteinases and TIMPs. New York: Oxford University Press; 2000.
[18] Turk BE, Huang LL, Piro ET, Cantley LC. Determination of protease cleavage site motifs using mixture-based oriented peptide libraries. Nat Biotechnol 2001;19(7):661–7.
[19] Chau Y, Tan FE, Langer R. Synthesis and characterization of dextran–peptide–methotrexate conjugates for tumor targeting via mediation by matrix metalloproteinase II and matrix metalloproteinase IX. Bioconjug Chem 2004;15(4):931–41.
[20] Ngan AHW, Wang HT, Tang B, Sze KY. Correcting power-law viscoelastic effects in elastic modulus measurement using depth-sensing indentation. Int J Solids Struct 2005;42(5–6):1831–46.
[21] Greenfield N, Fasman GD. Computed circular dichroism spectra for the evaluation of protein conformation. Biochemistry 1969;8:4108–16.
[22] Netzel-Arnett S, Sang QX, Moore WGI, Navre M, Birkedalhansen H, Vanwart HE. Comparative sequence specificities of human 72-kDa and 92-kDa gelatinases (type-IV collagenases) and pump (Matrilysin). Biochemistry 1993;32(25):6427–32.
[23] Rajagopal K, Schneider JP. Self-assembling peptides and proteins for nanotechnological applications. Curr Opin Struct Biol 2004;14(4):480–6.
[24] Yokoi H, Kinoshita T, Zhang SG. Dynamic reassembly of peptide RADA16 nanofiber scaffold. Proc Natl Acad Sci U S A 2005;102(24):8414–9.
[25] van Bommel KJ, Stuart MC, Feringa BL, van Esch J. Two-stage enzyme mediated drug release from LMWG hydrogels. Org Biomol Chem 2005;3(16):2917–20.
[26] van Bommel KJ, Friggeri A, Stuart M, Feringa BL, van Esch J. Protecting substrates from enzymatic cleavage: hydrogels of low molecular weight gelators do the trick. J Control Release 2005;101(1–3):287–90.
[27] Zhang SG, Holmes T, Lockshin C, Rich A. Spontaneous assembly of a self-complementary oligopeptide to form a stable macroscopic membrane. Proc Natl Acad Sci U S A 1993;90(8):3334–8.
[28] Werb Z. ECM and cell surface proteolysis: regulating cellular ecology. Cell 1997;91(4):439–42.
[29] Shofuda K, Moriyama K, Nishihashi A, Higashi S, Mizushima H, Yasumitsu H, et al. Role of tissue inhibitor of metalloproteinases-2 (TIMP-2) in regulation of progelatinase A activation catalyzed by membrane-type matrix metalloproteinase-1 (MT1-MRP) in human cancer cells. J Biochem 1998;124(2):462–70.
[30] Puyraimond A, Fridman R, Lemesle M, Arbeille B, Menashi S. MMP-2 colocalizes with caveolae on the surface of endothelial cells. Exp Cell Res 2001;262(1):28–36.